JOURNAL OF MATERIALS SCIENCE 13 (1978) 1709–1716

Expressions governing stress-strain curves in short fibre reinforced polymers

M. R. PIGGOTT
Department of Chemical Engineering and Applied Chemistry, University of Toronto, Toronto, Canada

The earlier theories of reinforcement for short fibre reinforced composites have been extended to include the estimation of strain as well as stress. Thus the effect on the stress–strain curve of various parameters can be estimated. It is shown that the shape of the stress–strain curve is strongly dependent on the fibre aspect ratio, while being relatively little affected by the adhesion between fibres and matrix. The coefficient of friction has an important effect on the stress–strain curve, and so also does the residual radial stress at the fibre–matrix interface. Unfortunately, little data is available at present on parameters such as friction, adhesion coefficients and residual and Poissons shrinkage stresses. Consequently, we are not yet in a position to design short fibre composites for high strength and modulus, coupled with optimum toughness.

1. Introduction

The early theories of fibre reinforcement give satisfactory explanations of either the failure strength, or the Young's modulus, but cannot be used for both at the same time. Thus Cox [1] considered elastic fibres reinforcing an elastic matrix, and assumed that the shears generated at the fibre–matrix interface could always be withstood. The stress–strain curve on this model is a straight line, ending when some failure mechanism supervenes. Tyson and Davies [2] showed that failure of Cox's stress transfer mechanism must occur at low applied stresses, since the shear stresses at the fibre–matrix interface become very high at the fibre end, even for very small applied stresses.

Dow [3] extended Cox's treatment to include matrices whose post-yield behaviour was governed by an approximately linear stress–strain curve, at a lower slope than in the elastic region. The matrix could thus be treated as though it had a second elastic constant. This, however, was still essentially an elasticity treatment, and hence, like Cox's, useful only for the prediction of elastic constants.

On the other hand, the frictional theory of Outwater [4], and the matrix flow theory described by Kelly and Davies [5] were developed in terms of stress only. Composite strains were not included in the equations, and consequently they can only be used for the estimation of the modulus. Similarly Piggott's [6] combination of the Cox and Kelly and Davies approaches was only used for the estimation of stresses.

The many texts on composite materials available today perpetuate this dichotomy, using the Cox theory, or improvements thereon, to show that with long fibres the Young's modulus of aligned fibre composites approaches the Law of Mixtures value, while for short fibres it falls below it by an amount depending on the fibre aspect ratio. The Outwater and/or Kelly and Davies approaches are used to show that composite strength varies with aspect ratio in a similar way. The incompatibility of the assumptions needed for the modulus expression and those needed for the strength expression never seem to have received any attention. (However, it should be noted that with very brittle matrices, the stress–strain curves have been explained theoretically [7]).

Composite materials are being used in the range of stresses between the very low stresses at which the Cox theory can be used, and the failure stresses described by the failure theories. Thus, some understanding of their behaviour in this region is required.

Recently, Piggott [8] showed that the various approaches described above could be reconciled, and governing equations for the whole stress–strain curve could be derived, both for reinforced metals, and polymers. The polymer case is described in detail here, and the importance of such factors as adhesion and friction at the interface are discussed for aligned fibre composites containing fibres of various lengths, or rather, aspect ratios. The significance of the results obtained for such other properties as toughness are also discussed.

2. Theory

2.1. General case

The theory previously appearing in synopsis form [8] will first be described. The forces between fibres and matrix are assumed to be symmetrical about the fibre centre, and interactions between adjacent fibres [9] are neglected. Thus we need consider only the fibre half-length, Fig. 1.

When the stresses applied to the composite are sufficiently low, there will be no slip between fibres and matrix. At high stresses slip occurs near the fibre ends. Let the length over which slip occurs be mL $(0 < m < 1)$ where L is the fibre half-length. The fibre tensile stress in this region, $\sigma_{fe}(x, \epsilon_m)$, will be a function of the distance x along the fibre, and matrix strain, ϵ_m. Let its average value be $\bar{\sigma}_{fe}(\epsilon_m)$ and its value at $x = L(1-m)$ be $\sigma_{fi}(\epsilon_m)$. Assume that no stress transfer occurs across the fibre ends, so that $\sigma_{fe} = 0$ at $x = L$.

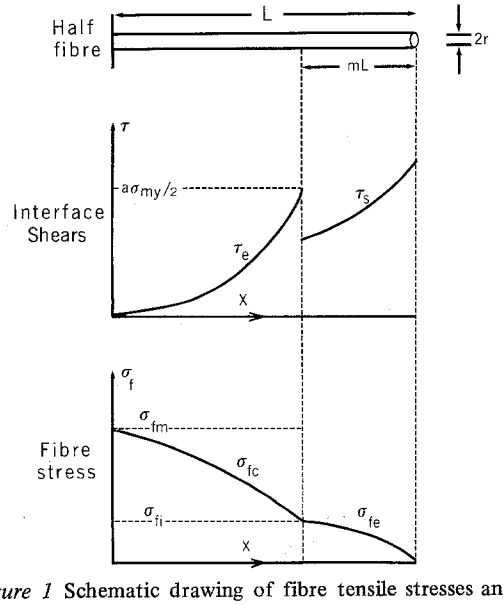

Figure 1 Schematic drawing of fibre tensile stresses and interfacial shears.

It is assumed that Cox's [1] treatment can be applied in the unslipped region, but that the shear forces at the fibre surface cannot exceed $a\sigma_{my}$, where a is an adhesion parameter (usually $0 < a < 1$) and σ_{my} is the matrix yield stress. Thus in this region the fibre stress, σ_{fc}, is governed by the equation

$$\frac{d^2\sigma_{fc}}{dx^2} = \frac{n^2}{r^2}(\sigma_{fc} - E_f\epsilon_m) \quad (1)$$

where r is the fibre radius and E_f is the Young's modulus of the fibre and

$$n^2 = 2E_m/[(1+\nu_m)E_f \ln(2\pi\sqrt{3}V_f)] \quad (2)$$

for hexagonally packed fibres. Here E_m is the Young's modulus and ν_m the Poisson's ratio for the matrix. V_f is the fibre volume fraction.

We can integrate Equation 1 with the boundary conditions $\sigma_{fc} = \sigma_{fi}$ at $x = L(1-m)$, remembering that the stresses are symmetrical about the fibre mid-point. Thus for $x < L(1-m)$

$$\sigma_{fc} = E_f\epsilon_m + [\sigma_{fi}(\epsilon_m) - E_f\epsilon_m]\cosh\left(\frac{nx}{r}\right)/\cosh n\bar{s} \quad (3)$$

where

$$\bar{s} = \frac{L}{r}(1-m) \quad (4)$$

ϵ_m is determined by differentiating Equation 3 and putting $d\sigma_{fc}/dx = -a\sigma_{my}/r$ at $x = L(1-m)$. Thus

$$\epsilon_m = \left[\sigma_{fi}(\epsilon_m) + \frac{a\sigma_{my}}{n}\coth n\bar{s}\right]/E_f \quad (5)$$

Substituting Equation 5 into Equation 3 gives

$$\sigma_{fc} = \sigma_{fi}(\epsilon_m) + \frac{a\sigma_{my}}{n}\left[\coth n\bar{s} - \cosh\left(\frac{nx}{r}\right)/\sinh n\bar{s}\right] \quad (6)$$

for $x < L(1-m)$. The maximum fibre stress, σ_{fm}, is at $x = 0$:

$$\sigma_{fm} = \sigma_{fi}(\epsilon_m) + \frac{a\sigma_{my}}{n}\tanh\left(\frac{n\bar{s}}{2}\right) \quad (7)$$

The average fibre stress, $\bar{\sigma}_f$, is obtained by integration:

$$\bar{\sigma}_f = \frac{1}{L}\int_0^{L(1-m)} \sigma_{fc}\,dx + m\bar{\sigma}_{fe}(\epsilon_m) \quad (8)$$

$$= a\sigma_{my}[(1-m)\coth n\bar{s} - 1/ns]/n + (1-m)\sigma_{fi}(\epsilon_m) + m\sigma_{fe}(\epsilon_m) \quad (9)$$

where s is the aspect ratio of the fibres, L/r. Finally, the composite stress, σ_c, is given by

$$\sigma_c = V_f\bar{\sigma}_f + (1-V_f)E_m\epsilon_m \quad (10)$$

Stress–strain curves may be plotted by substitution of appropriate values of m into Equations 5 and 9, and calculation of σ_c using Equation 10. The loci of the curves depend very strongly on the assumptions made about the mode of stress transfer near the fibre ends (these determine $\sigma_{fi}(\epsilon_m)$ and $\bar{\sigma}_{fe}(\epsilon_m)$).

2.2. Fibre reinforced polymers

For reinforced polymers it is usually assumed that the high stresses at the fibre–matrix interface near the fibre ends result in failure of the bond between fibres and matrix. Sliding of the fibres relative to the matrix can then occur, and this phenomenon has recently been examined in detail under conditions such that the matrix was under stress, as in stressed composites [10]. The sliding process was found to be governed by frictional forces which are themselves controlled by matrix and fibre contractions arising from Poisson's ratio effects, together with residual contractions due, for example, to curing.

The Poisson's contractions inside a composite have not been evaluated. Theoretical treatments yield results which do not even make it possible to decide, for a given volume fraction of fibres, whether the interfacial stresses are tensile or compressive [11]. The short fibre case is more complicated than the continuous fibre case, and the only available formula for this [11] is unacceptable, since it tends to infinity as the volume fraction of fibre goes to zero, and in any case considers only one fibre, surrounded by a block of pure matrix material.

We need terms which independently allow for the matrix contractions and the fibre contractions near their ends. These contractions are shown schematically in Fig. 2. In order to avoid complication at this stage, these will be expressed by the simplest possible parameters.

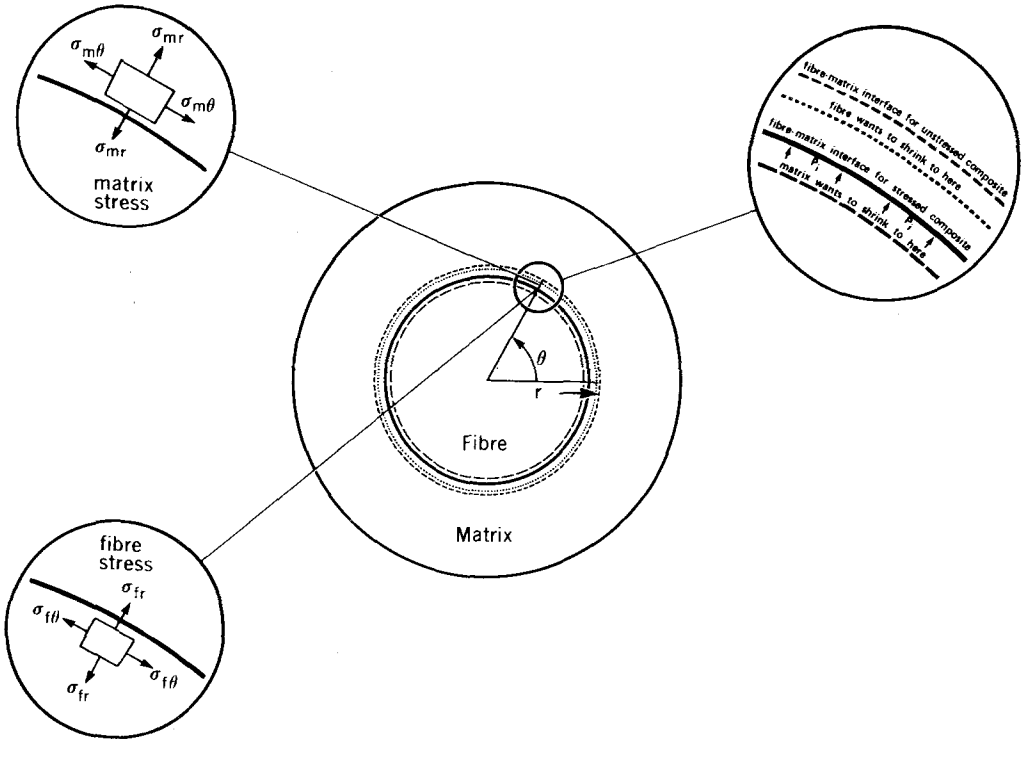

Figure 2 Schematic view of radial displacements of matrix, fibre, and the fibre–matrix interface. The small elements indicate the stress in the fibres and matrix at the interface.

Consider the matrix first. When a tube of matrix is stressed axially, and contracts against a rigid liner, a simple elasticity treatment shows that the interfacial radial stress is $-\nu_m \sigma_m/(1+\nu_m)$. (The minus sign indicates that the stress is compressive). In a composite, the situation is a good deal more complex, but we could evidently express the stress in the form $-\nu_1 \sigma_m$ where ν_1 must depend on the Poisson's ratio of the matrix, but is likely also to be affected by fibre volume fraction, and the elastic moduli of fibres and matrix. The prior work already quoted [11] indicates that its value may not be very different from ν_m.

Superposed on this stress will be the residual stress, σ_r, due to cure shrinkage of the matrix, or differential thermal expansion of the fibres and matrix during manufacture.

The fibre strain, due to its Poisson's contraction, is $\nu_f \sigma_f/E_f$. Such a strain, if acting alone, and if translated directly into matrix strain at the fibre–matrix interface, would give rise to an interfacial stress $\nu_f \sigma_f E_m/E_f$. If we replace ν_f by ν_2, we have a simple parameter which can be used to describe this contraction, and by analogy with ν_1, can be expected to depend principally on ν_f, but also to be affected by the volume fraction and elastic moduli. Its value is not likely to be very different from ν_f.

These stresses can be superposed. Thus the normal stress at the fibre surface, σ_{rt}, may be expressed by the equation

$$\sigma_{rt} = -\nu_1 \sigma_m + \nu_2 \sigma_{fe} E_m/E_f + \sigma_r \quad (11)$$

The fibre stress in the end region is governed by friction and may be obtained from

$$\frac{d\sigma_{fe}}{dx} = \frac{2\mu}{r}\sigma_{rt} = \frac{2\mu}{r}(-\nu_1 \sigma_m + \nu_2 \sigma_{fe} E_m/E_f + \sigma_r) \quad (12)$$

where μ is the coefficient of friction. By integration of Equation 12 with $\sigma_{fe} = 0$ when $x = L$, and $\sigma_m = E_m \epsilon_m$ we obtain

$$\sigma_{fe} = \frac{E_f(\nu_1 E_m \epsilon_m - \sigma_r)}{E_m \nu_2}\{1 - \exp(-2\mu\nu_2 E_m(L-x)/E_f r)\} \quad (13)$$

Writing

$$p = 2\mu\nu_2 ms E_m/E_f \quad (14)$$

and remembering that σ_{fi} is σ_{fe} when $x = L(1-m)$ we can eliminate σ_{fi} and ϵ_m in turn between Equations 5 and 13 to obtain

$$\epsilon_m = \frac{a\nu_2 \sigma_{my} \coth(n\bar{s})/nE_f - \sigma_r(1-e^{-p})/E_m}{\nu_2 - \nu_1(1-e^{-p})} \quad (15)$$

$$\sigma_{fi} = \frac{a\nu_1 \sigma_{my} \coth(n\bar{s})/n - \sigma_r E_f(1-e^{-p})/E_m}{\nu_2 - \nu_1(1-e^{-p})} \quad (16)$$

Finally, the value of $\bar{\sigma}_{fe}$ may be found by integration of Equation 13 between the limits $x = L(1-m)$ and $x = L$, and division by mL;

$$\bar{\sigma}_{fe} = \sigma_{fi}\left(\frac{1}{1-e^{-p}} - \frac{1}{p}\right) \quad (17)$$

3. Stress–strain curves predicted

We are now in a position to examine the effect on the stress–strain curves of the various parameters.

3.1. The effect of aspect ratio

If the toughness of a composite is to be maximized by using short fibres, it is most important to know what effect this will have on modulus and strength, and on the stress–strain curve.

We will consider a stiff graphite fibre reinforced epoxy. We will use the values of μ and σ_r found by Hadjis and Piggott [10] for steel in epoxy, since this appears to be the most nearly relevant test. Thus $\mu = 0.19$ and $\sigma_r = 3.0$ MPa. We will assume that $\nu_1 = \nu_m/(1+\nu_m)$, the expression normally used for the contraction of a very thick walled tube of matrix, and that ν_2 is given with sufficient accuracy by $\nu_2 = \nu_f/(1+\nu_m)$. (For a discussion of suitable values for ν_1 and ν_2, and the effect of changing them, see Section 3.5.) The adhesion parameter, a, will have the value 1.0, for maximum possible adhesion.

Fig. 3 shows stress–strain curves for the graphite-epoxy for aspect ratios ranging from 30 to 10000. The curves have been terminated at the fibre breaking point, or at about 1% strain if the fibres do not break. The continuous curves

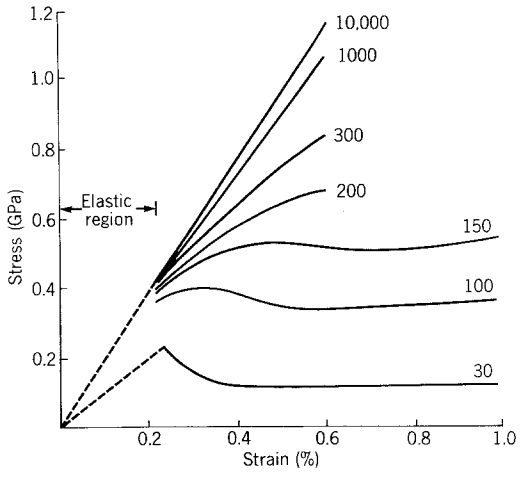

Figure 3 Effect of aspect ratio on stress–strain curves of short carbon fibre reinforced epoxy resin with $V_f = 0.5$. The solid curves start at the elastic limit, and the labels on the curves give the fibre aspect ratios.

start at the completion of the elastic deformation, i.e., when adhesion failure occurs, and the fibres start sliding in the matrix. (During the elastic stage, the stress–strain curve is linear, of course, and the dashed lines are used to illustrate this region.) The relevant fibre and matrix data are given in Table I.

The curves show the expected tendency towards the Law of Mixtures expression:

$$E_c = V_f E_f + (1-V_f)E_m \qquad (18)$$

as the aspect ratio becomes large. A 10% deviation from the Law of Mixtures is obtained for an aspect ratio of 1000, while, when the aspect ratio is 10 000, the deviation becomes insignificant. The critical aspect ratio is somewhere between 150 and 200, since the fibres break when $s = 200$ and do not when $s = 150$. There is a yield drop for the aspect ratio of 150, which becomes severe at lower aspect ratios.

The composite strength never achieves the Law of Mixtures value, even when the aspect ratio tends to infinity. This is because the breaking strain of the matrix, $\epsilon_{mu} = 0.028$, exceeds that of the fibres, $\epsilon_{fu} = 0.0061$. The matrix thus carries a stress $E_m \epsilon_{fu}$ at the instant of fibre failure, for $s \to \infty$. Thus, instead of the Law of Mixtures for composite strength, σ_{cu}, we have

$$\sigma_{cu} = V_f \sigma_{fu} + V_m E_m \epsilon_{fu} \qquad (19)$$

This result is already well established.

TABLE I Properties of fibres and matrix used for calculation of theoretical curves

Material	Young's modulus (GPa)	Poisson's ratio	Yield strength (GPa)
Carbon fibres	377	0.16	2.3*
Epoxy resin	2.5	0.34	0.060

*Tensile strength.
All curves were drawn for a volume fraction of each component of 0.5.

3.2. The effect of the adhesion

The adhesion parameter a, if varied between 0 and 1, can be used to describe the effect of extremely good adhesion or very poor adhesion as well as intermediate values. When $a = 1$ the interface fails at the matrix yield stress. This might be regarded as perfect adhesion, since when the adhesion is strong enough (i.e., stronger than the matrix itself), matrix failure will occur at or near the interface near the fibre end, once the applied stress has reached a high enough value. At the other end of the scale, $a = 0.001$ represents a very weak bond. For example, an epoxy resin will yield at a shear stress of about 35 MPa. Thus, when $a = 0.001$, for an epoxy the adhesive fails at 35 kPa; this is indeed weak.

Fig. 4 shows the effect of varying the adhesion parameter, a, for a number of aspect ratios. The effect of the adhesion is very small, except at low aspect ratios, and even when the aspect ratio is only 30, it merely smooths out the curve. The curves are drawn for good adhesion ($a = 1$) and vanishingly small adhesion ($a = 0.001$). Intermediate values fall between these limits. The other constants are as in Fig. 3.

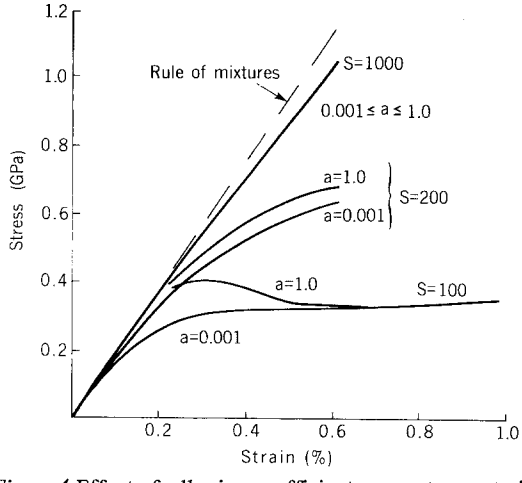

Figure 4 Effect of adhesion coefficient, a, on stress–strain curves for carbon-epoxy, for fibre aspect ratios (s) of 100, 200 and 1000, and $V_f = 0.5$. (For $s = 1000$ the curves for $a = 1.0$ and $a = 0.001$ are coincident).

The most significant effect of a is on the elastic limit. Equation 9 reduces to

$$\bar{\sigma}_f = a\sigma_{my}\left(\coth ns - \frac{1}{ns}\right)\Big/n \qquad (20)$$

when $m = 0$, i.e., at the elastic limit. Thus the average fibre stress at this point is directly proportional to the adhesion parameter.

3.3. The effect of residual stresses

Fig. 5 shows the effect of varying the residual stress, σ_r, at an aspect ratio of 200. All the other constants are as in Fig. 3.

It is clear that the residual stress should be large and compressive for efficient reinforcement. If it is too small there is a danger of a large yield drop. Even with an aspect ratio of 1000, the stress drops to 70 MPa at a strain of 0.55% (but subsequently rises again to 540 MPa at 1% strain) when there is no residual stress. The critical aspect ratio appears to be affected by the residual stress, since the fibres do not break when it is −10 MPa, though they do when it is −30 MPa.

If the residual stress is tensile, there is great danger of complete failure at the yield stress. No stress transfer can occur in the fibre end regions when

$$v_1 E_m \epsilon_m - \sigma_r < 0 \qquad (21)$$

since otherwise Equation 12 would give a negative value for σ_{fc}, indicating that complete separation is occurring at the fibre–matrix interface.

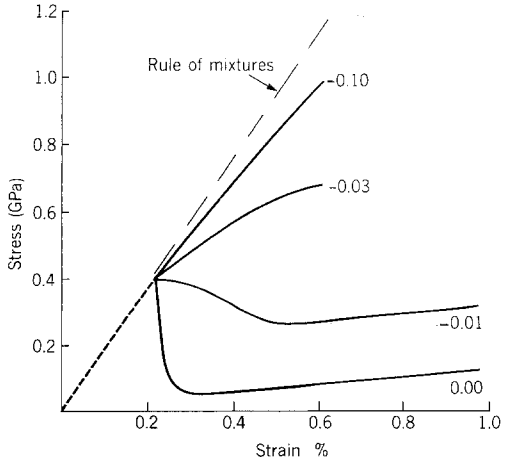

Figure 5 Effect of residual stress on the stress–strain curve for carbon-epoxy for a fibre aspect ratio of 200 and $V_f = 0.5$. The solid curves start at the elastic limit, and the labels on the curves give the residual stress, the negative sign indicating compression.

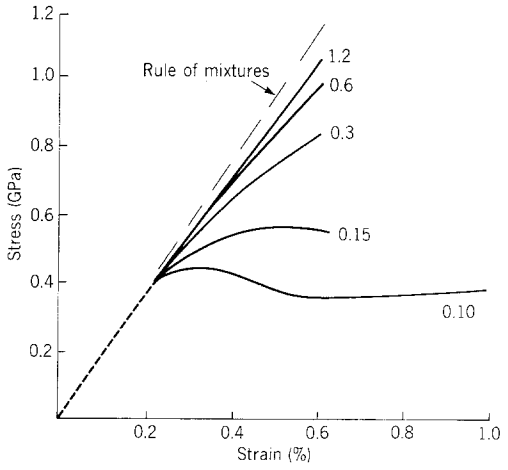

Figure 6 Effect of friction coefficient on the stress–strain curve for carbon-epoxy for a fibre aspect ratio of 200 and $V_f = 0.5$. The solid curves start at the elastic limit, and the labels on the curves give the friction coefficient.

At the yield point, $\epsilon_m = 0.23\%$ for the carbon-epoxy. Inserting this value into Equation 21, together with the other data for the composite, we find that the residual stress must be less than +1.4 MPa. If the residual stress is tensile, and greater than this, reinforcement does not take place beyond the yield point of the material, no matter how large the aspect ratio is.

3.4. Effect of friction

Fig. 6 shows the effect of varying the coefficient of friction, μ, at an aspect ratio of 200. When $\mu = 0.1$, the critical aspect ratio is greater than 200, since the fibres do not break. The critical aspect ratio appears to be approximately 200 when $\mu = 0.15$.

3.5. Effect of matrix and fibre shrinkage coefficients

In the absence of reliable data on the radial stresses at the fibre–matrix interface, an approximate evaluation of the effect of certain assumptions about the radial stresses will be made.

We will assume that near the end of a fibre the composite acts as a thick walled tube, surrounding the fibre, and exerting a pressure p_i on it. Let the outer radius of the tube be R and the inner radius r, the Young's modulus E and the Poisson's ratio ν.

The interfacial shear stress will be assumed to act along the fibre direction only. Thus, although it affects the matrix and fibre axial stresses, σ_m and σ_f, it will not affect the matrix radial and

circumferential stresses, σ_{mr} and $\sigma_{m\theta}$, or the fibre radial and circumferential stresses σ_{fr} and $\sigma_{f\theta}$ (see Fig. 2).

The stresses at the inner wall of the tube can be evaluated from equations given by Timoshenko and Goodier [12]:

$$\sigma_{mr} = -p_i \tag{22}$$

$$\sigma_{m\theta} = \frac{R^2 + r^2}{R^2 - r^2} p_i = bp_i \tag{23}$$

where

$$b = (R^2 + r^2)/(R^2 - r^2) \tag{24}$$

The radial displacement at the inner wall due to the pressure is $rp_i(b + \nu)/E$, so, superimposing the Poisson's contraction due to the axial stress, i.e., $-\nu\sigma_m r/E$, we obtain, for the total radial displacement, u_{mr},

$$u_{mr} = r[p_i(b + \nu) - \nu\sigma_m]/E \tag{25}$$

Similarly, the stresses in the fibre may be calculated, and come to

$$\sigma_{fr} = \sigma_{f\theta} = -p_i \tag{26}$$

Since this is a state of uniform compression, we may use the fibre radial strain to calculate the displacement directly. Thus, applying Hooke's Law, the fibre radial strain, ϵ_{fr}, is given by

$$\epsilon_{fr} = -[\nu_f\sigma_f + (1 - \nu_f)p_i]/E_f \tag{27}$$

and the displacement is $r\epsilon_{fr}$.

Since the radial displacements must be equal as long as contact is maintained between fibres and matrix, we have

$$p_i = \frac{\nu\sigma_m - \nu_f\sigma_f E/E_f}{1 + b\nu + (1 - \nu_f)E_m/E_f} \tag{28}$$

This is very similar to the Mooney and McGarry [13] equation for the continuous non-densely packed fibre case, if we let $E = E_m$, $\nu = \nu_m$, and $b \gg a$. This is because, for continuous fibres $\sigma_f/E_f = \sigma_m/E_m$, and the equation reduces to

$$p_i = \frac{\sigma_m(\nu_m - \nu_f)}{1 + \nu_m + (1 - \nu_f)E_m/E_f} \tag{29}$$

For fibre reinforced polymers $E_m \gg E_f$, so that Equation 28 reduces, for $b \gg a$, to

$$p_i = \frac{\nu_m}{1 + \nu_m}\sigma_m - \frac{\nu_f E_m}{E_f(1 + \nu_m)}\sigma_f \tag{30}$$

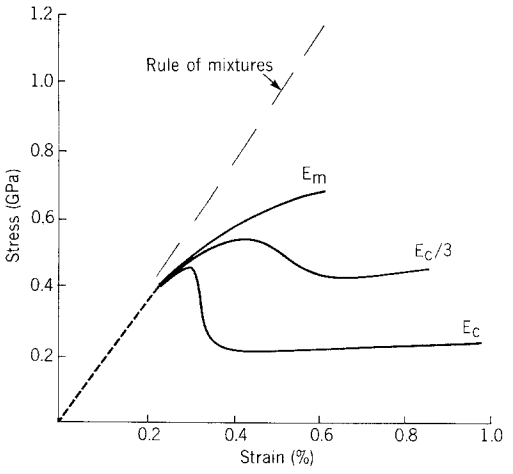

Figure 7 Effect of Poisson's contractions on the stress–strain curve for carbon epoxy for a fibre aspect ratio of 200 and $V_f = 0.5$. The Poisson contractions are strongly dependent on the value of E chosen (see Equation 28) and the curves are drawn for minimum and maximum possible values of E, and one intermediate value.

The values of ν_1 and ν_2 used in Section 3.1 are in accordance with this equation, and thus in keeping with the Mooney and McGarry equation for $E_m \ll E_f$.

For short fibre reinforced composites, however, it may be more appropriate to equate E with E_c rather than with E_m. For large volume fractions, this affects the result very considerably, as can be seen in Fig. 7. Here the effect of varying E from E_m to E_c, for $s = 200$ and $V_f = 0.5$ is shown. The reduced matrix contractions resulting from the larger values of E increase the yield drop effect and increase the critical aspect ratio.

4. Discussion

It has been shown than it is possible to extend Outwater's theory of reinforcement by friction to include the evaluation of composite strains, and the effect of matrix and fibre contractions. Thus stress–strain curves can now be predicted for fibre reinforced polymers, and these show the following features.

(1) Using realistic values for such parameters as the coefficient of friction, the high aspect ratios needed for reinforced polymers are clearly demonstrated. For example, with carbon fibre reinforced epoxy the critical aspect ratio is at least 150 and efficient reinforcement requires that the aspect ratio should be at least 1000.

(2) Adhesion does not appear to have a very

large effect on the shape of the stress–strain curve. Although it affects the elastic limit to a marked extent, efficient reinforcement can be obtained with high aspect ratios (1000 or more) with vanishingly small adhesion ($a = 0.001$).

(3) Residual stresses are very important. Short fibre composites can only be used at high stress levels (i.e., levels beyond the elastic limit) when the residual stresses are relatively large and compressive. Otherwise large yield drops are predicted, and the composite could, in consequence, fail suddenly at the elastic limit. The combination of poor adhesion and low residual stress appears to be particularly dangerous, since in this case the elastic limit is at low stress, and yielding could thus occur at low applied stress.

(4) The coefficient of friction is an important parameter, and has a large effect on the stress–strain curve for short fibres.

Unfortunately, information on the parameters affecting the stress–strain curve is scanty. Although a lot of work on pull-out has been carried out, very little of it has been done under conditions where the friction coefficient can be estimated. Clearly, much further work is needed here.

Moreover, there is a marked lack of published data on stress–strain curves for well-characterized, short, aligned fibre reinforced polymers. The stress–strain curves predicted by the theory do, however, fit in with the general observation that short fibre composites do not have such good mechanical properties as continuous fibre reinforced ones.

Still another parameter on which information is scanty is the radial stress in composites. The theoretical treatments do not give definite results for a given volume fraction, and even the sign of these stresses is open to question. While experimental results for shear stresses are abundant, those for radial stresses are not.

It is important that we have this data so that the critical aspect ratio can be predicted. Short fibre composites have an important role in the spectrum of materials. Reinforced thermoplastics often have short fibres for ease of processing (extrusion etc.) and this is also true of some reinforced thermosets. To obtain the best results for strength and modulus it is necessary to know the critical aspect ratio, so that conditions can be optimized to ensure that the aspect ratio in the finished composite is at least five to ten times this value.

In addition, for advanced composites, where toughness is important, it is often desirable to have the aspect ratio no more than five times the critical value [14]. This can obviously only be done when data is available which will permit the estimation of the critical aspect ratio.

Clearly, a great deal more work needs to be done before the design of short fibre composites can be carried out on a rational basis.

References

1. H. L. COX, *Brit. J. Appl. Phys.* **3** (1952) 72.
2. W. R. TYSON and G. J. DAVIES, *ibid.* **16** (1965) 199.
3. N. F. DOW, G. E. Report #R635E61 (1963).
4. J. OUTWATER, *Modern Plastics.* **33** (1956) 37.
5. A. KELLY and G. J. DAVIES, *Met. Rev.* **10** (1965) 37.
6. M. R. PIGGOTT, *Acta Met.* **14** (1966) 1429.
7. J. AVESTON, G. A. COOPER and A. KELLY, NPL Conference of Properties of Fibre Composites (IPC Sci. Tech. Press, Guildford, 1971) p.15.
8. M. R. PIGGOTT, *Proc. ICCM.* **2** (Boston, 1976) 1322.
9. V. R. RILEY, *J. Comp. Mater.* **2** (1968) 436.
10. N. HADJIS and M. R. PIGGOTT, *J. Mater. Sci.* **12** (1977) 358.
11. G. S. HOLISTER and C. THOMAS, "Fibre Reinforced Materials" (Elsevier, London, 1969) p. 49.
12. S. TIMOSHENKO and J. N. GOODIER, "Theory of Elasticity" (McGraw–Hill, London, 1951) p. 60.
13. R. D. MOONEY and F. J. McGARRY, Proceedings of the 14th Conference of the SPI Reinforced Plastics Division (1959) Section 12E.
14. M. R. PIGGOTT, *J. Mater. Sci.* **9** (1974) 494.

Received 30 September and accepted 15 December 1977.